Experimental section

Chemicals and materials

Zinc sulfate ($ZnSO_4$) was supplied by Shanghai Macklin Biochemical Technology Co., Ltd. Potassium bicarbonate ($KHCO_3$) was purchased from Tianjin Damao Chemical Reagent Factory. Potassium chloride (KCl) was sourced from Tianjin Huirui Chemical Technology Co., Ltd. Hydrochloric acid (HCl, 36~38%), ethanol and sulfuric acid (H_2SO_4, 95~98%) were provided by Guangdong Fine Chemical Engineering Technology Research and Development Center. Lactic acid ($C_3H_6O_3$, 85~90%) was supplied by Beijing Innochem Science & Technology Co., Ltd. Sodium hydroxide (NaOH) were obtained from Tianjin Fengchuan Chemical Reagent Technology Co., Ltd. Bare Zn foil (0.2 mm thickness) and Nafion N-117 proton exchange membrane (0.18 mm thickness, exchange capacity ≥0.92 meq/g) were supplied by Alfa Aesar (China) Chemical Co., Ltd. Acetonitrile (MeCN) was purchased from Tianjin Fuyu Fine Chemical Co., Ltd. Ionic liquids including 1-butyl-3-methylimidazolium hexafluorophosphate ([Bmim]PF_6), 1-butyl-3-methylimidazolium trifluoromethanesulfonate ([Bmim]OTf), 1-butyl-3-methylimidazolium perchlorate ([Bmim]ClO_4), and 1-butyl-3-methylimidazolium dicyanamide ([Bmim]$N(CN)_2$) were obtained from the Center for Green Chemistry and Catalysis, Lanzhou Institute of Chemical Physics, Chinese Academy of Sciences. High-purity carbon dioxide (CO_2, 99.999%) and high-purity nitrogen (N_2, 99.999%) were supplied by Henan Yumeng Technology Co., Ltd.

The synthetic method of the ZnO-pc/Zn electrode

The ZnO pre-catalyst was prepared following a previously reported method.[40] Prior to use, the bare Zn was sequentially polished with sandpaper and ultrasonically cleaned in water and ethanol to remove surface oxides and impurities. The cleaned Zn foil was then electrochemically activated via cyclic voltammetry (CV) scans from -1.5 V to 1.5 V *vs.* Ag/AgCl for 7 cycles at 50 $mV\cdot s^{-1}$ in 0.1 M $KHCO_3$ and 4 mM KCl solution, to further purify the surface and increase its specific surface area. Subsequently, the ZnO pre-catalyst was grown on the pre-treated bare Zn to form the ZnO-pc/Zn electrode via a facile electrochemical deposition route. First, the electrolyte was prepared by dissolving 2.42 g of $ZnSO_4$ in a mixture of 9 mL lactic acid and 50 mL H_2O. Then, under continuous stirring in an ice bath, 6.4 g of NaOH was slowly added to the solution until a uniform white suspension was obtained. For the electrodeposition, the pre-treated bare Zn served as the working electrode, with a Pt mesh as the counter electrode and an Ag/AgCl electrode as the reference. The process was conducted in the prepared suspension at 60 °C under continuous stirring, applying a constant current density of -20 $mA\cdot cm^{-2}$ for 1 h to obtain the final ZnO-pc/Zn electrode.

Synthetic methods of r-ZnO-pc/Zn-CO_2 and r-ZnO-pc/Zn-N_2 electrodes

The r-ZnO-pc/Zn-CO_2 and r-ZnO-pc/Zn-N_2 electrodes were synthesized via an electrochemical reduction method. The reduction was conducted in an H-type cell with a standard three-electrode system, comprising the ZnO-pc/Zn electrode as the working electrode, a Pt mesh as the counter electrode, and an Ag/Ag^+ electrode as the reference. Prior to reduction, the electrolyte (30 wt% [Bmim]PF_6/MeCN/5 wt% H_2O) was saturated with either CO_2 or N_2 gas for 30 min through continuous bubbling. Subsequently, the electrochemical reduction was performed at an applied potential of -3.0 V *vs.* Ag/Ag^+ for 1 h. The resulting electrodes treated under CO_2 and N_2 atmospheres were designated as r-ZnO-pc/Zn-CO_2 and r-ZnO-pc/Zn-N_2 electrodes, respectively.

Characterizations

The morphologies and structures of r-ZnO-pc/Zn-CO_2, r-ZnO-pc/Zn-N_2, ZnO-pc/Zn, and bare Zn electrodes were characterized by SEM (Care Zeiss SIGMA 500). TEM and elemental mapping images of r-ZnO-pc/Zn-CO_2 and r-ZnO-pc/Zn-N_2 samples were conducted on a Tecnai G2 F20 TEM equipped with an energy-dispersive X-ray spectroscopy (EDS) system. The crystalline phases of r-ZnO-pc/Zn-CO_2, r-ZnO-pc/Zn-N_2, ZnO-pc/Zn, and bare Zn electrodes were identified by XRD using an X'pert PRO diffractometer with Cu-Kα radiation (λ = 0.15406 nm) at a scanning rate of $5°\cdot min^{-1}$. The surface chemical composition and valence states of the r-ZnO-pc/Zn-CO_2 and r-ZnO-pc/Zn-N_2 electrodes were investigated by XPS on a Thermo Scientific ESCALAB 250Xi spectrometer with the binding energy calibrated to the C 1s peak at 284.8 eV. XANES measurements on r-ZnO-pc/Zn-CO_2, ZnO-pc/Zn, ZnO, and Zn foil were conducted at the 1W2B beamline of the Beijing Synchrotron Radiation Facility, with the acquired XAFS data analyzed using the ATHENA program.

The eCO_2RR test and the product analysis

The eCO_2RR tests were conducted in an H-type cell with a CHI 6081E electrochemical workstation. The three-electrode system consisted of a Pt mesh counter electrode, an Ag/Ag^+ reference electrode, and working electrode (r-ZnO-pc/Zn-CO_2, r-ZnO-pc/Zn-N_2, ZnO-pc/Zn, or bare Zn electrodes). The anode and cathode compartments were separated by a Nafion-117 proton exchange membrane. The catholyte was 30 mL of 30 wt% [Bmim]PF_6/MeCN/5 wt% H_2O, while the anolyte was 30 mL of 0.5 M H_2SO_4 aqueous solution. Prior to electrolysis, the catholyte was purged with CO_2 for 30 min at a constant flow rate of $20\ mL\cdot min^{-1}$ under continuous stirring. The LSV curves were performed in the CO_2- or N_2-saturated catholyte by scanning the potential from -1.2 V to -2.5 V *vs.* Ag/Ag^+ at a rate of $20\ mV\cdot s^{-1}$. Potentiostatic electrolysis experiments were conducted at a series of applied potentials (-1.7 V, -1.8 V, -1.9 V, -2.0 V, -2.1 V, -2.2 V, and -2.3 V *vs.* Ag/Ag^+). The electrolysis time was 1 h. Following electrolysis, gaseous products were analyzed using an Agilent 8860 GC equipped with TCD and FID detectors, while liquid products were characterized by ^1H NMR spectroscopy (Bruker Avance III 600 HD). The EIS measurement was performed on the r-ZnO-pc/Zn-CO_2 and r-ZnO-pc/Zn-N_2 electrodes at OCP in the 30 wt% [Bmim]PF_6/MeCN/5 wt% H_2O electrolyte using a 5 mV amplitude and a frequency range of $10^{-2} \sim 10^6$ Hz. The ECSA was estimated by determining the C_{dl} value, which was achieved by measuring CV curves for the r-ZnO-pc/Zn-CO_2, r-ZnO-pc/Zn-N_2, and bare Zn electrodes at various scan rates ($20 \sim 90\ mV\cdot s^{-1}$) within a non-faradaic potential window (-1.45 V ~ -1.75 V *vs.* Ag/Ag^+). The C_{dl} values were then obtained from the slope of the plot of current density difference (Δj) at -1.6 V *vs.* Ag/Ag^+ versus scan rate.

In-situ attenuated total reflection surface-enhanced infrared reflection spectroscopy (ATR-SEIRS) measurements

In-situ electrochemical ATR-SEIRAS experiments were conducted using a PerkinElmer Spectrum3 Fourier transform infrared spectrometer equipped with a liquid-nitrogen-cooled mercury-cadmium-telluride (MCT) detector. A gold-coated silicon prism served as both the infrared-reflective substrate and the catalyst support, functioning as the working electrode. The catalyst powders were scraped off the r-ZnO-pc/Zn-CO_2 electrode surface. An Ag/Ag^+ electrode and a platinum mesh were employed as the reference and counter electrodes, respectively. The electrolyte was CO_2-saturated 30 wt%-[Bmim]PF_6/MeCN/5 wt%-H_2O. All data were collected with a spectral resolution of $4\ cm^{-1}$. In-situ ATR-SEIRAS spectra were recorded in real time at different applied potentials using a potential-stepping method.

Supplementary Figures

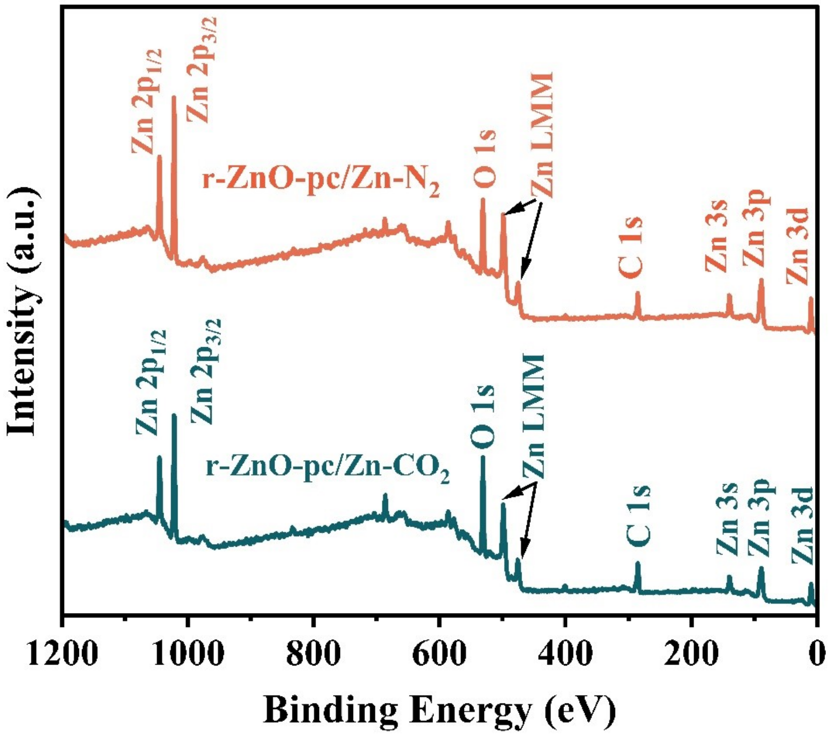

Fig. S1 The XPS survey spectra of r-ZnO-pc/Zn-CO$_2$ and r-ZnO-pc/Zn-N$_2$ electrodes.

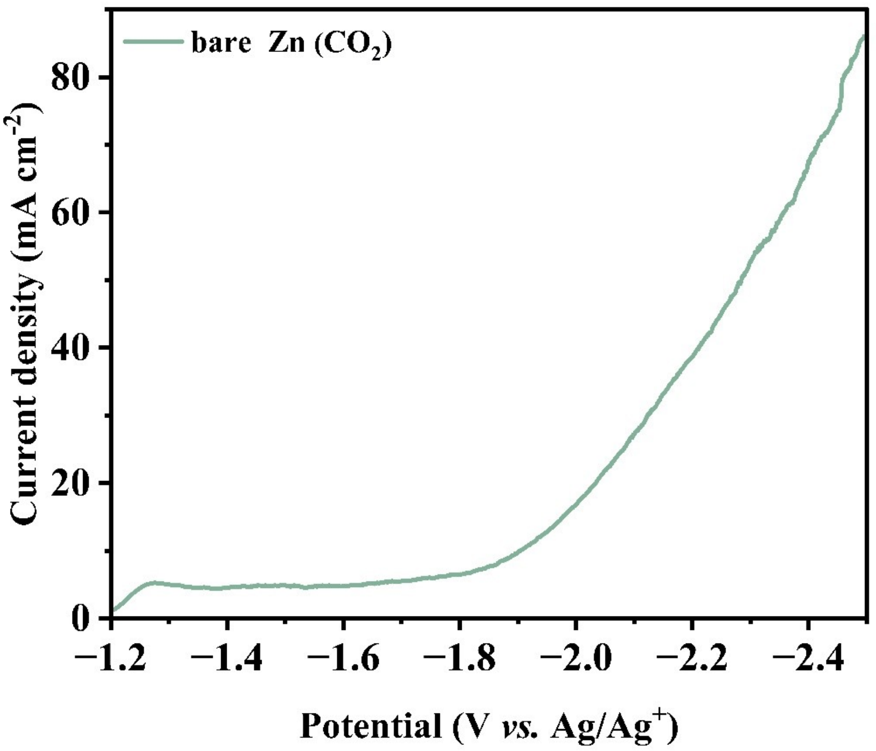

Fig. S2 The LSV curve for the bare Zn electrode in the CO_2-saturated 30 wt%-[Bmim]PF_6/MeCN/5 wt%-H_2O electrolyte.

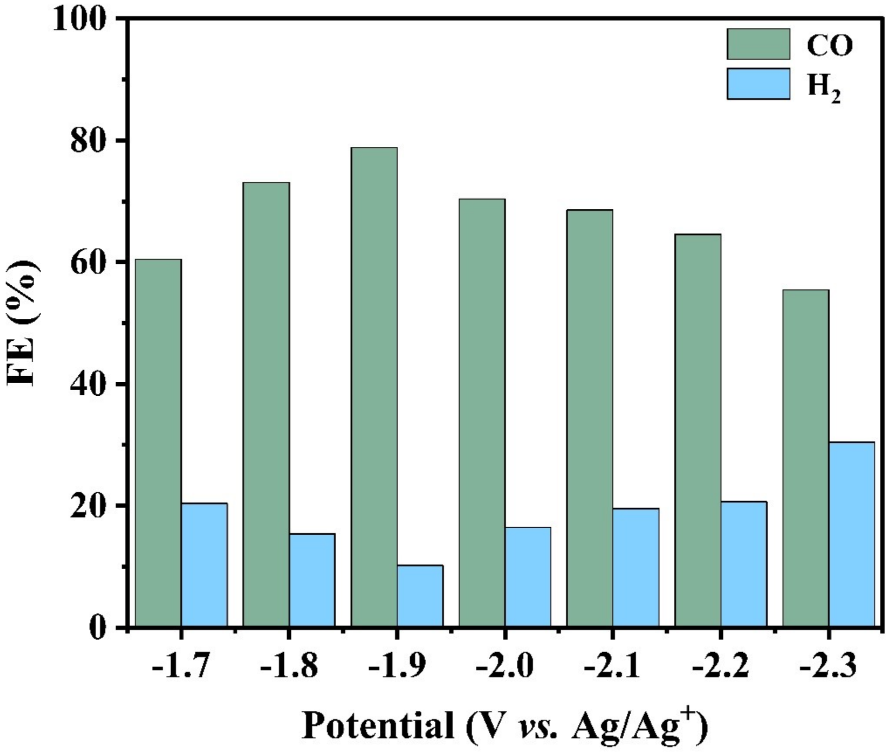

Fig. S3 FEs of CO and H_2 at different applied potentials on the bare Zn electrode. The electrolysis time was 1 h.

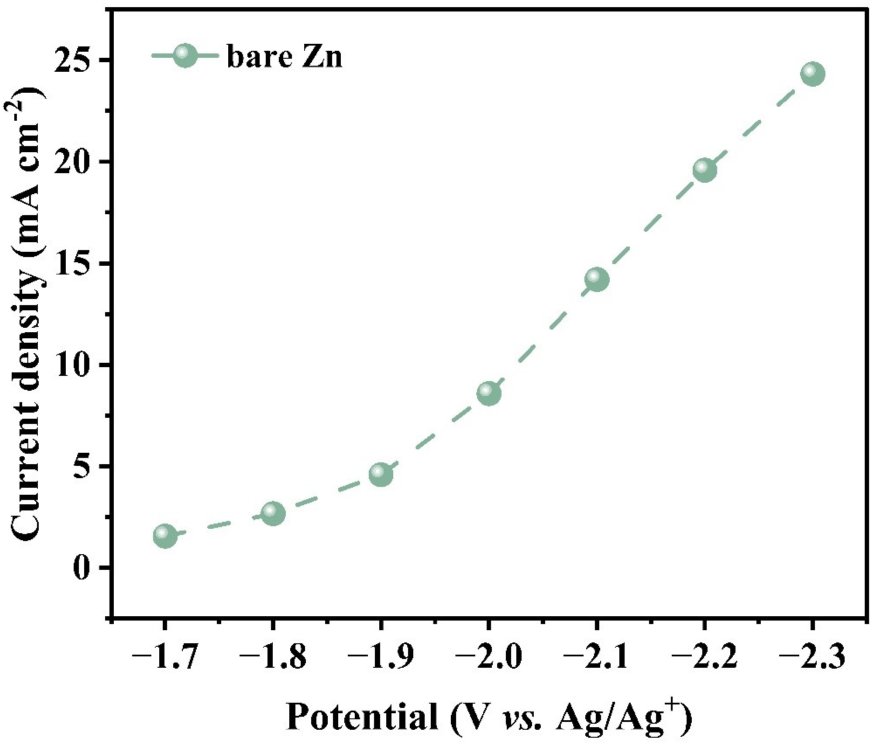

Fig. S4 Current densities at different applied potentials over the bare Zn electrode. The electrolysis time was 1 h.

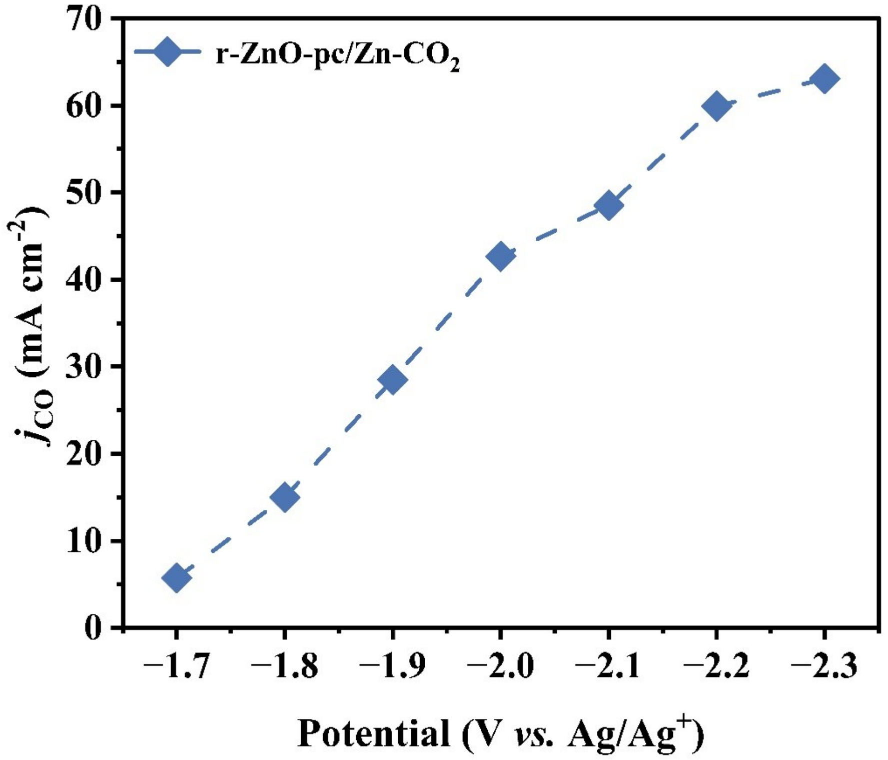

Fig. S5 The j_{CO} of the r-ZnO-pc/Zn-CO$_2$ electrode at different applied potentials. The electrolysis time was 1 h.

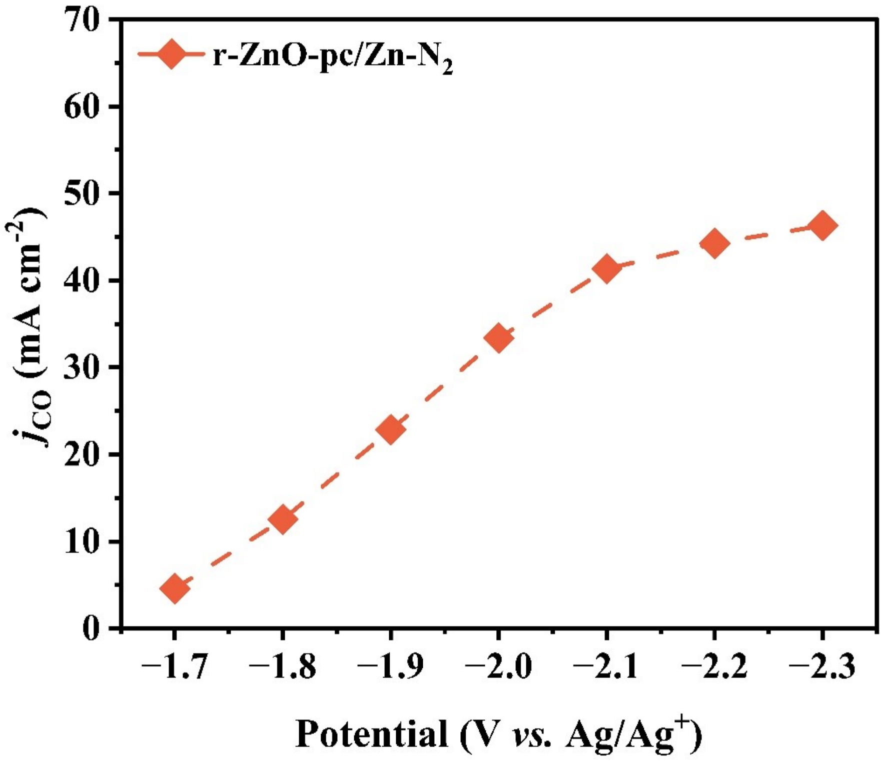

Fig. S6 The j_{CO} of the r-ZnO-pc/Zn-N_2 electrode at different applied potentials. The electrolysis time was 1 h.

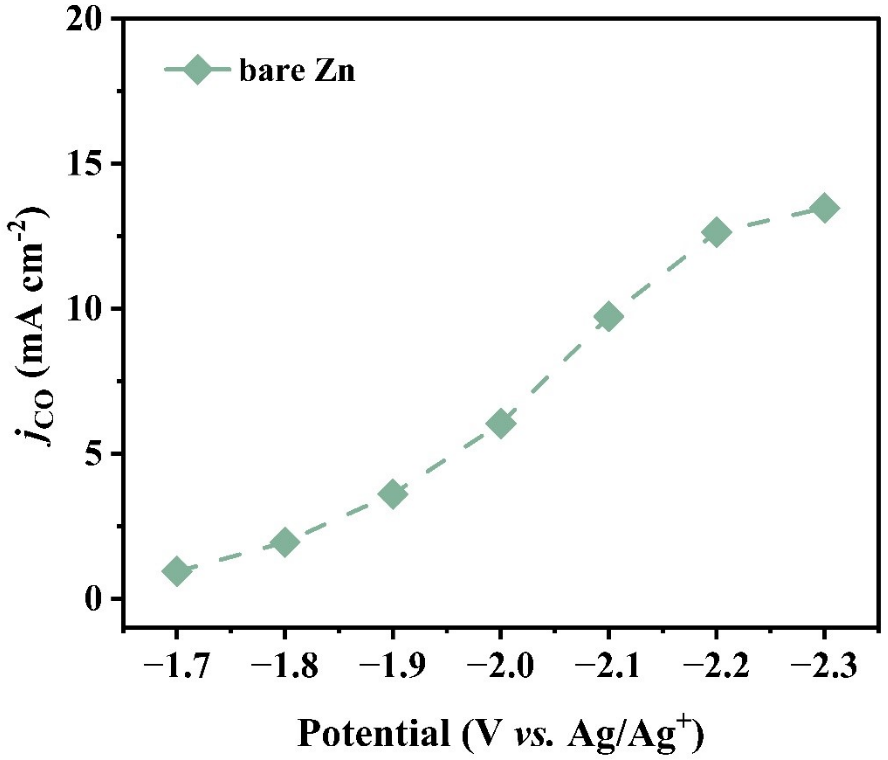

Fig. S7 The j_{CO} of the bare Zn electrode at different applied potentials. The electrolysis time was 1 h.

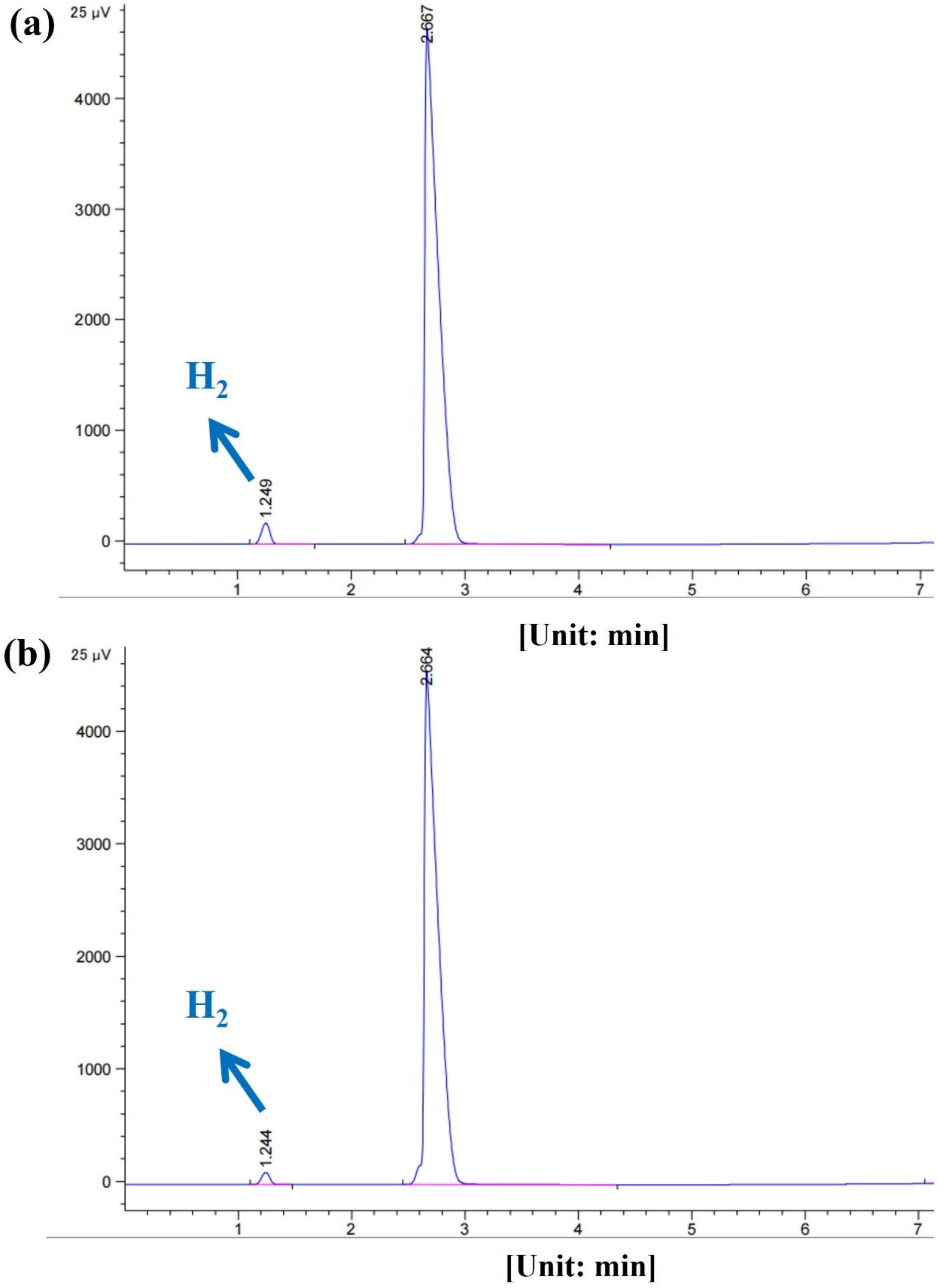

Fig. S8 GC spectra for gaseous products on (a) r-ZnO-pc/Zn-CO_2 and (b) r-ZnO-pc/Zn-N_2 electrodes in N_2-saturated electrolytes. The electrolysis time was 1 h.

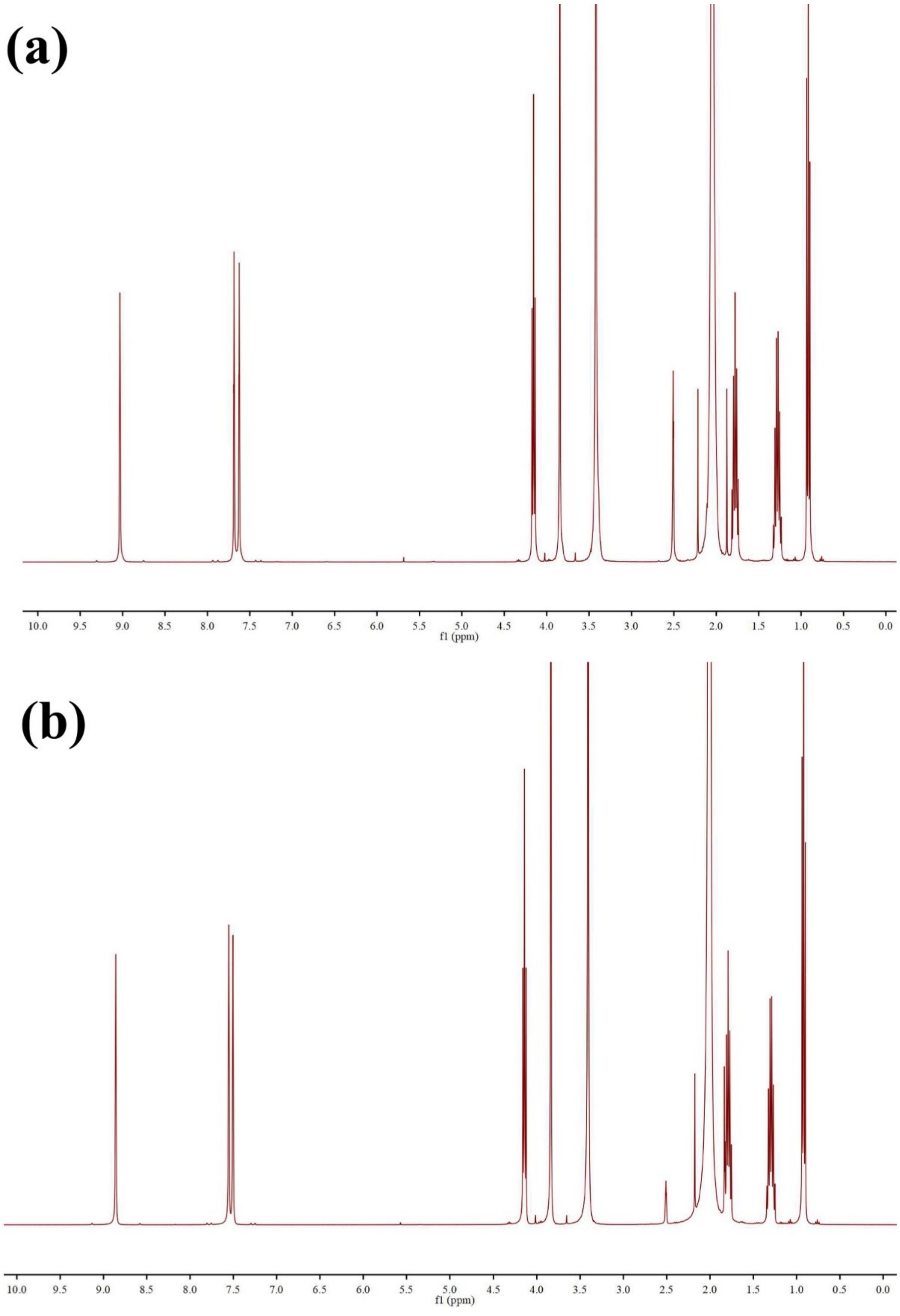

Fig. S9 ^{1}H NMR spectra for liquid products on (a) r-ZnO-pc/Zn-CO_2 and (b) r-ZnO-pc/Zn-N_2 electrodes in N_2-saturated electrolytes. The electrolysis time was 1 h.

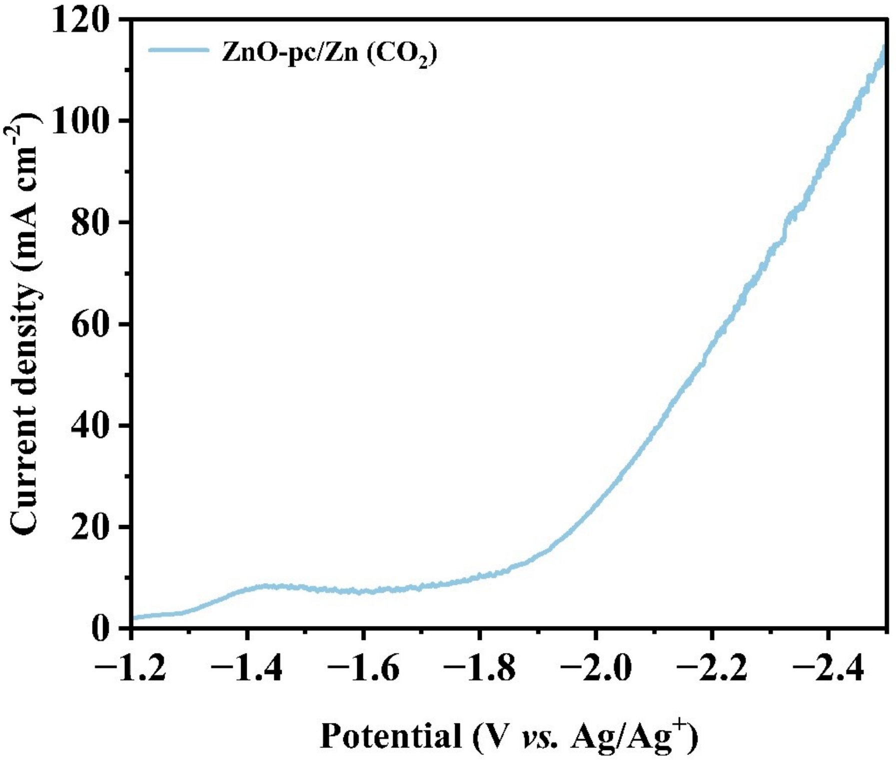

Fig. S10 The LSV curve for the ZnO-pc/Zn electrode in CO_2-saturated 30 wt%-[Bmim]PF_6/MeCN/5 wt%-H_2O electrolytes.

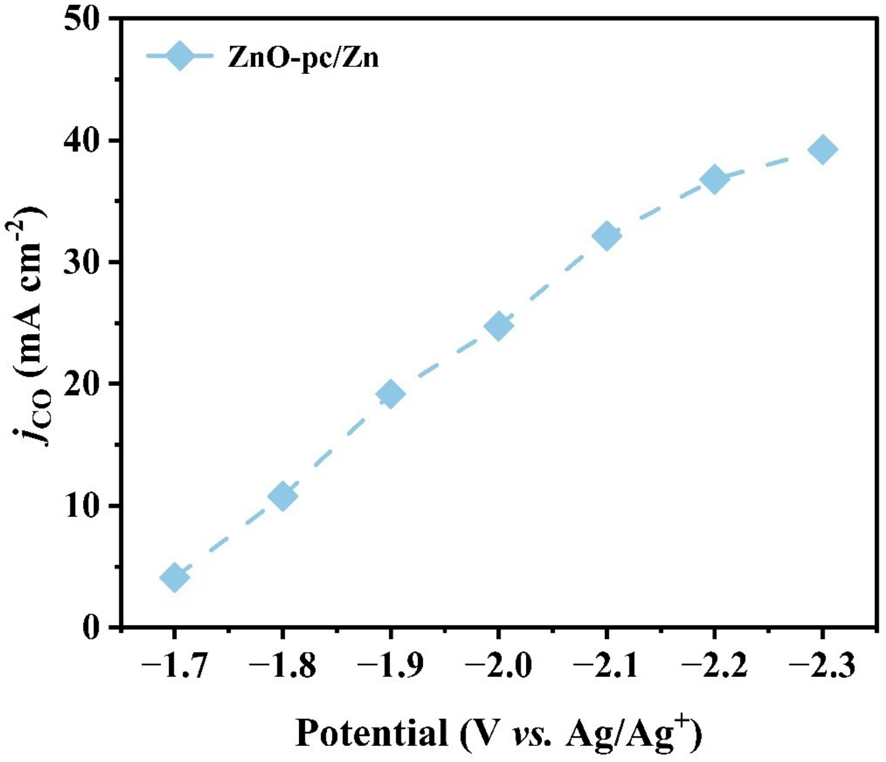

Fig. S11 The j_{CO} of the ZnO-pc/Zn electrode at different applied potentials. The electrolysis time was 1 h.

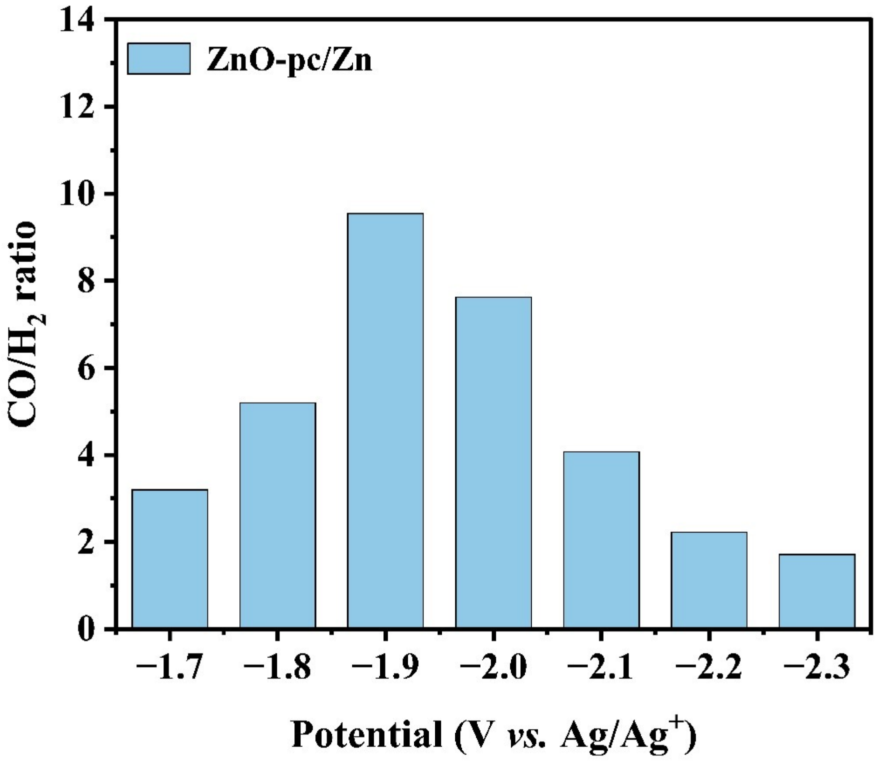

Fig. S12 The CO/H_2 ratios on the ZnO-pc/Zn electrode at different applied potentials. The electrolysis time was 1 h.

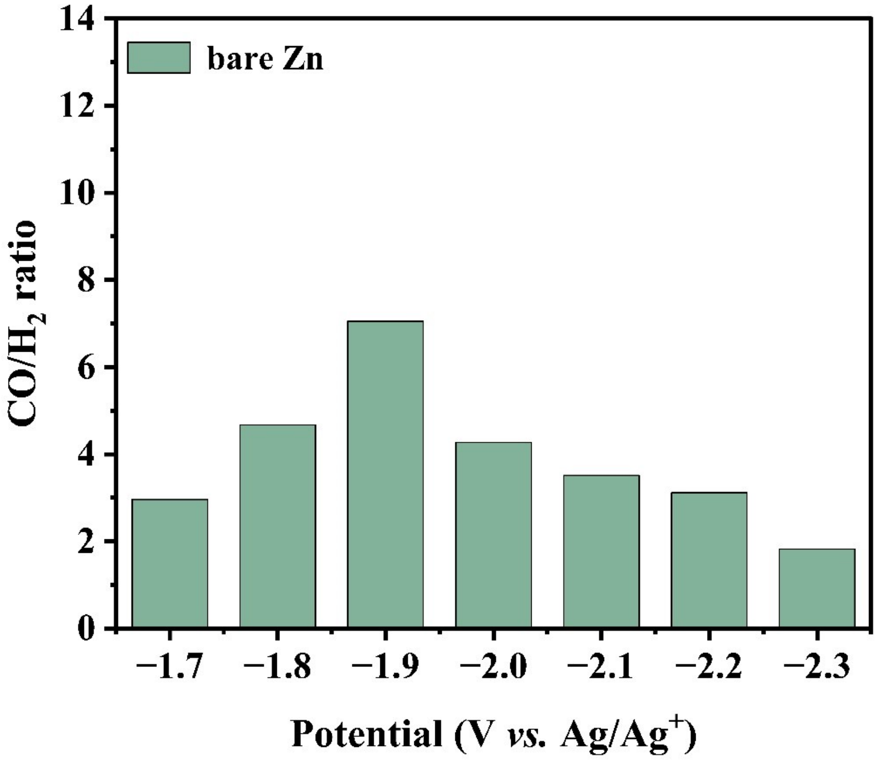

Fig. S13 The CO/H_2 ratios on the bare Zn electrode at different applied potentials. The electrolysis time was 1 h.

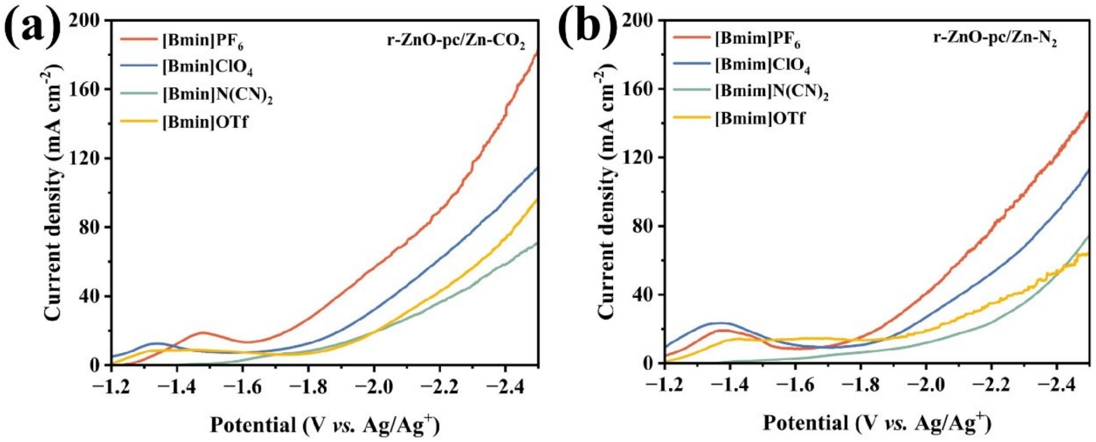

Fig. S14 LSV curves for different electrodes in CO_2-saturated electrolytes containing different ionic liquids: (a) r-ZnO-pc/Zn-CO_2 and (b) ZnO-pc/Zn-N_2 electrodes.

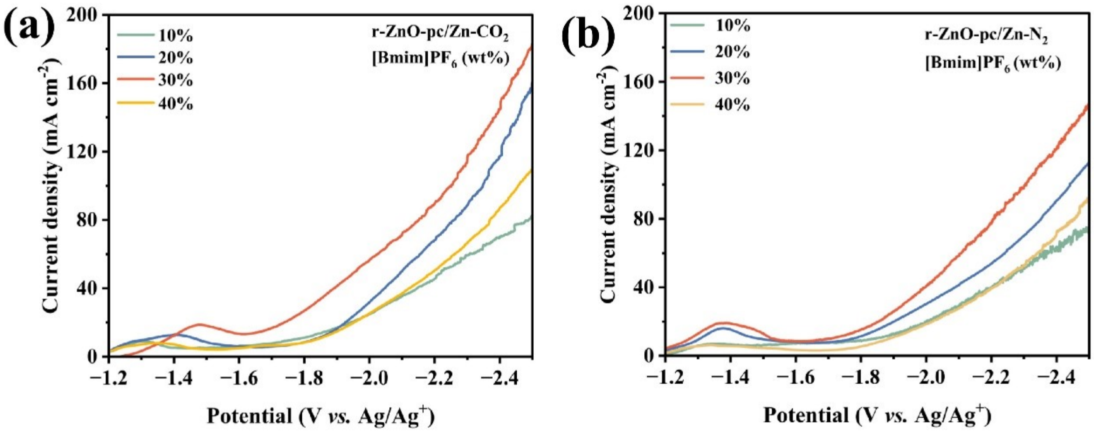

Fig. S15 LSV curves for different electrodes in CO_2-saturated $[Bmim]PF_6$/MeCN/5 wt%-H_2O electrolytes with different $[Bmim]PF_6$ concentrations: (a) r-ZnO-pc/Zn-CO_2 and (b) ZnO-pc/Zn-N_2 electrodes.

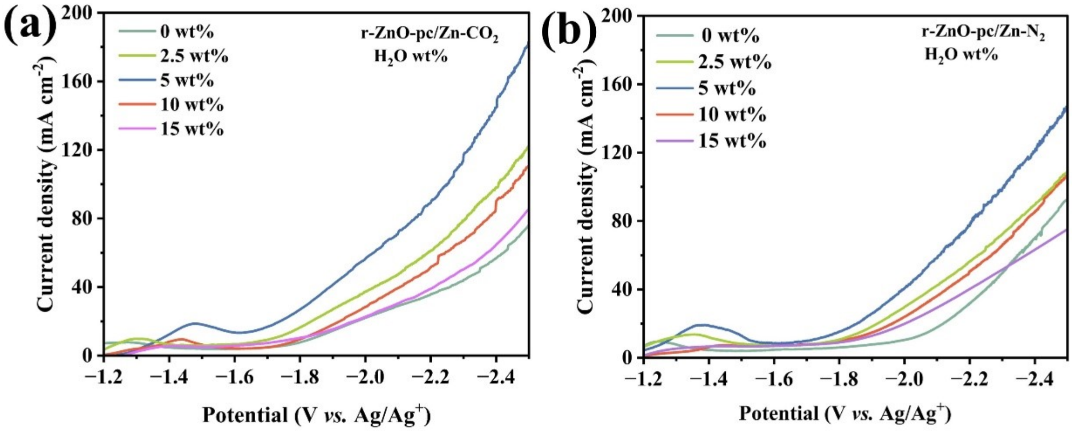

Fig. S16 LSV curves for different electrodes in CO_2-saturated 30 wt%-[Bmim]PF_6/MeCN/H_2O electrolytes with different H_2O contents: (a) r-ZnO-pc/Zn-CO_2 and (b) ZnO-pc/Zn-N_2 electrodes.

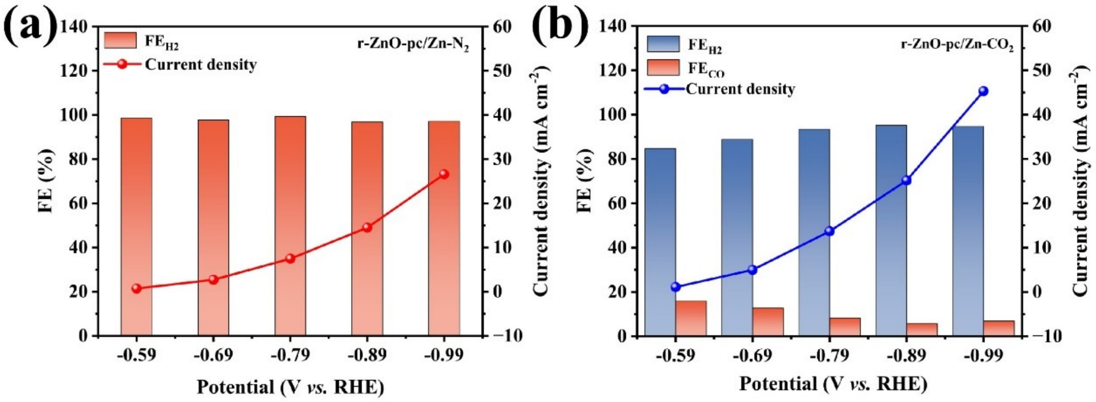

Fig. S17 FEs of different products and current density at various applied potentials on different electrodes in 1 M $KHCO_3$ solution: (a) r-ZnO-pc/Zn-N_2 and (b) r-ZnO-pc/Zn-CO_2 electrodes. The electrolysis time was 1 h.

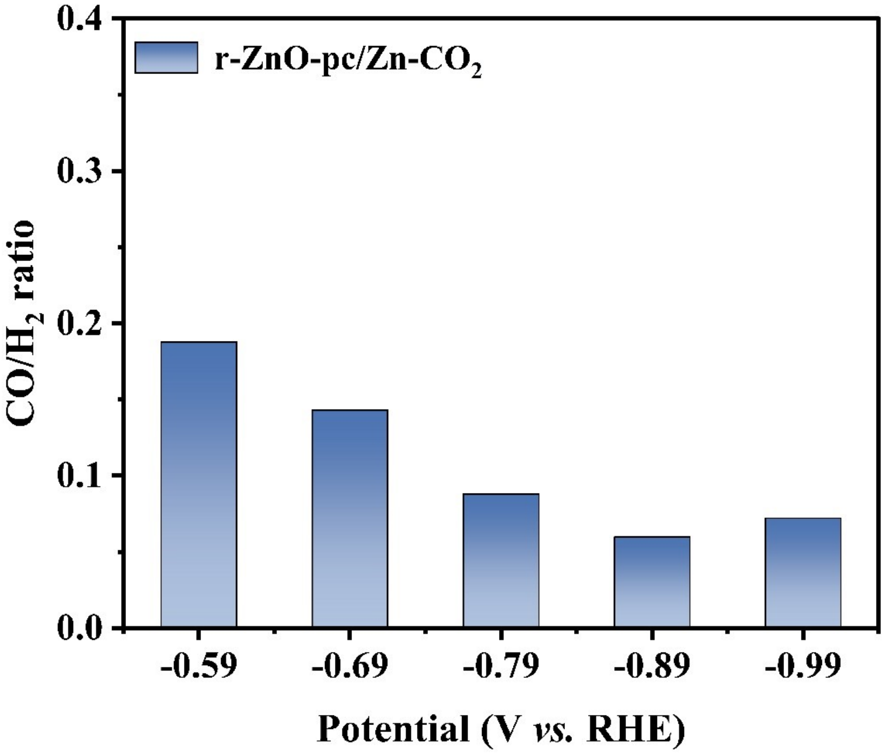

Fig. S18 The CO/H_2 ratios on r-ZnO-pc/Zn-CO_2 electrodes at different applied potentials in 1 M $KHCO_3$ solution. The electrolysis time was 1 h.

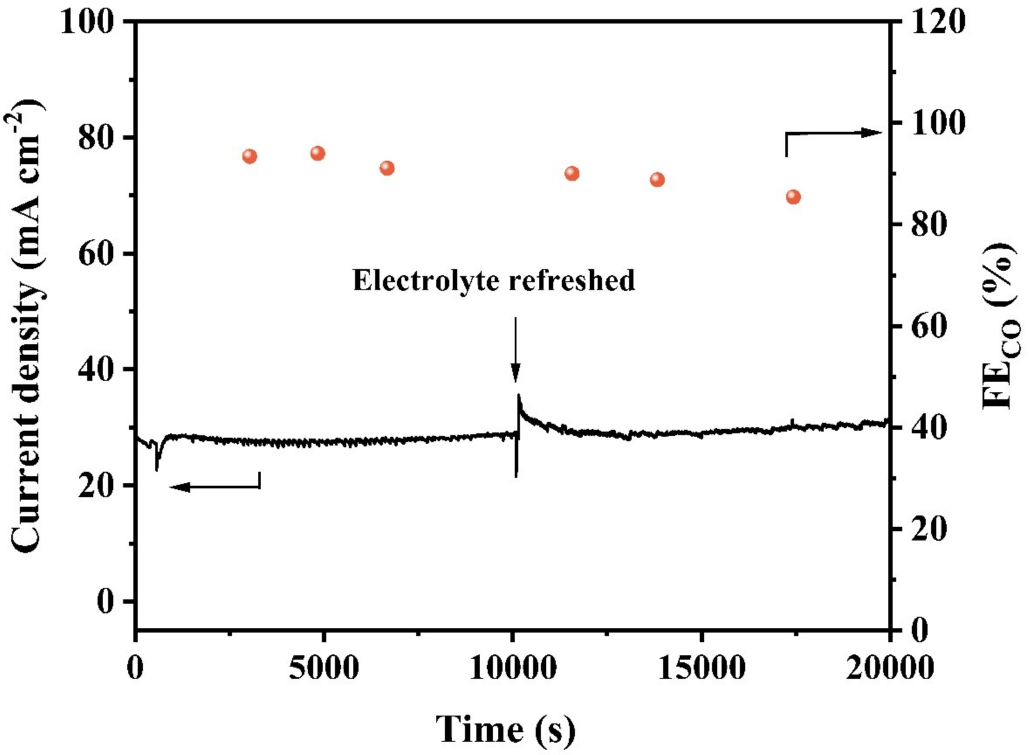

Fig. S19 The long-term stability test of the r-ZnO-pc/Zn-CO_2 electrode in the 30 wt%-[Bmim]PF_6/MeCN/5 wt%-H_2O electrolyte at -1.9 V *vs.* Ag/Ag^+.

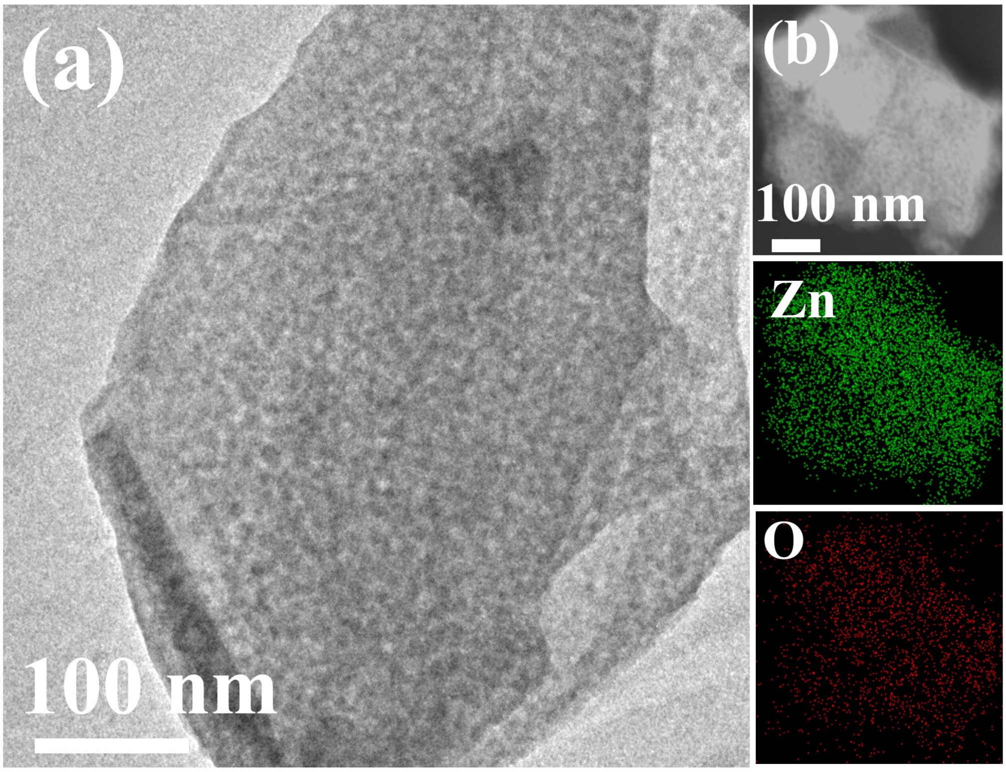

Fig. S20 (a) TEM image and (b) elemental mapping images of the used r-ZnO-pc/Zn-CO_2 electrode.

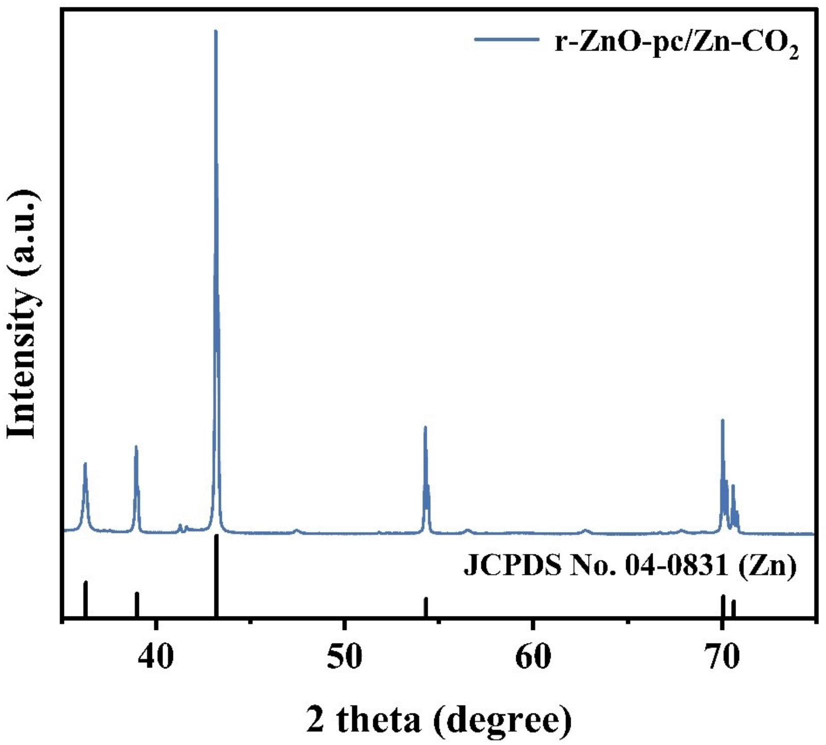

Fig. S21 The XRD pattern of the used r-ZnO-pc/Zn-CO_2 electrode.

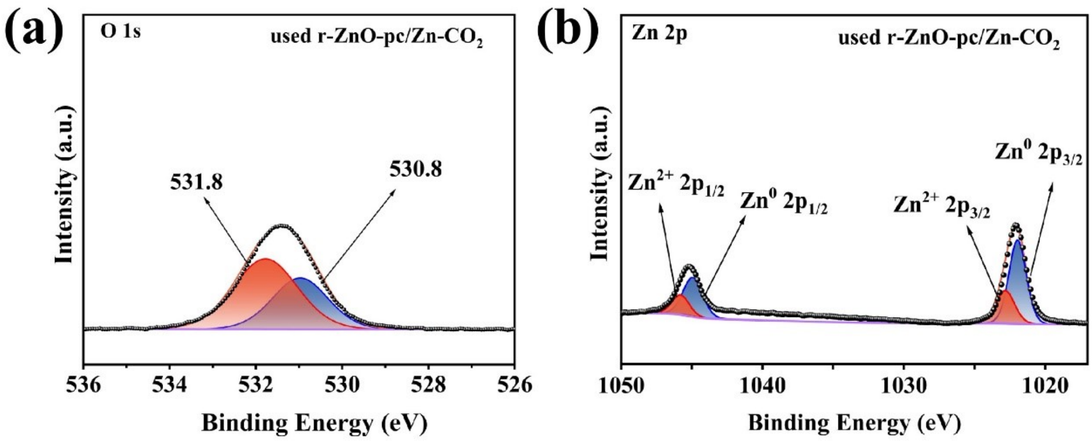

Fig. S22 High-resolution XPS spectra of the used r-ZnO-pc/Zn-CO$_2$ electrodes: (a) O 1s and (b) Zn 2p.

Table S1. The eCO_2RR-to-syngas performance for recently reported Zn-based catalysts, r-ZnO-pc/Zn-CO_2, and r-ZnO-pc/Zn-N_2 electrodes.

Catalyst	Electrolyte	Electrolytic cell	Potential	Current Density (mA cm^{-2})	Range of CO/H_2 ratios	FE_{CO} (%)	Ref.
Zn Al-LDO	0.1 M $KHCO_3$	H type	-1.3 V *vs.* RHE	10.05	0.01 ~ 1.45	59.12	9
Cd-ZIF-8	0.1 M $KHCO_3$	H type	-1.1 V *vs.* RHE	5	0.33 ~ 4	78	10
ZnO doped carbon	0.5 M $KHCO_3$	H type	-1.2 V *vs.* RHE	27.07	0.67 ~ 2.7	71	38
Zn-film	0.5 M $KHCO_3$	H type	-0.97 V *vs.* RHE	35.3	0.09 ~ 11.4	92.6	39
Co_xZn_γ-ZIFs	0.5 M $KHCO_3$	H type	-0.9 V *vs.* RHE	26	1 ~ 4	~35	59
Cu-ZnO	0.1 M $KHCO_3$	H type	-1.2 V *vs.* RHE	42.36	0.38 ~ 3.22	75.62	60
Cu-Zn bimetallic	0.1 M $KHCO_3$	H type	-0.81 V *vs.* RHE	~5	0.6 ~ 2.1	55.9	61
CuZn-2	0.1 M KOH	H type	-1.08 V *vs.* RHE	10	0.8 ~ 5.8	54.4	62
ZnAl-LDH	0.1 M $KHCO_3$	H type	-1.4 V *vs.* RHE	65	0.32 ~ 1.35	48	63
$Cu_{0.07}Zn$	0.1 M $KHCO_3$	H type	-0.95 V *vs.* RHE	20	1.1 ~ 4.3	77.3	64
AuZn/ZnO	0.1 M $KHCO_3$	H type	-0.9 V *vs.* RHE	1.9	0.25 ~ 2.5	66.4	65
CZN-0.5	0.1 M $KHCO_3$	H type	-1.0 V *vs.* RHE	~10	0.24 ~ 2.82	68	66
ZnO@f	0.5 M $KHCO_3$	H type	-1.2 V *vs.* RHE	24.4	0.5 ~ 2.7	71	67

Cu/Zn HF	0.5 M $KHCO_3$	H type	-0.92 V *vs.* RHE	~200	1 ~ 3.2	76.2	68
Zn cNS-HF	0.5 M KCl	H type	-1.3 V *vs.* RHE	73.3	0.4 ~ 3	62	69
r-ZnO-pc/Zn-N_2	30 wt%-$[Bmim]PF_6$/MeCN/5 wt%-H_2O	H type	-1.9 V *vs.* Ag/Ag^+	23.7	0.8 ~ 9.8	92.5	This work
r-ZnO-pc/Zn-CO_2	30 wt%-$[Bmim]PF_6$/MeCN/5 wt%-H_2O	H type	-1.9 V *vs.* Ag/Ag^+	28.9	0.8 ~ 12.5	98.6	This work
r-ZnO-pc/Zn-CO_2	30 wt%-$[Bmim]PF_6$/MeCN/5 wt%-H_2O	H type	-2.2 V *vs.* Ag/Ag^+	115.8	~1	51.7	This work